

Single top quark production as a probe of anomalous $tq\gamma$ and tqZ couplings at the FCC-ee

Hamzeh Khanpour^{1,2,3}, Sara Khatibi¹, Morteza Khatiri Yanehsari^{1,4},
Mojtaba Mohammadi Najafabadi¹

¹ *School of Particles and Accelerators, Institute for Research in Fundamental Sciences (IPM) P.O. Box 19395-5531, Tehran, Iran*

² *Farhangian University, Shariati Branch, P.O.Box 48491-11167, Sari, Mazandaran, Iran*

³ *Department of Physics, Faculty of Basic Sciences, Babol University of Technology, P.O.Box 47148-71167, Babol, Iran*

⁴ *Department of Physics, Ferdowsi University of Mashhad, P.O. Box 1436, Mashhad, Iran*

Abstract

In this paper, a detailed study to probe the top quark flavour-changing neutral currents $tq\gamma$ and tqZ at the future e^-e^+ collider FCC-ee/TLEP in three different center-of-mass energies of 240, 350 and 500 GeV is presented. A set of useful variables are proposed and used in a multivariate technique to separate signal $e^-e^+ \rightarrow Z/\gamma \rightarrow t\bar{q}$ ($\bar{t}q$) from standard model background events. The 3σ discovery regions and the upper limits on the FCNC branching ratios at 95% C.L in terms of the integrated luminosity are presented. It is shown that with 100 fb^{-1} of integrated luminosity of data, FCC-ee would be able to exclude the effective coupling strengths above $\mathcal{O}(10^{-4} - 10^{-5})$ which is corresponding to branching fraction of $\mathcal{O}(0.01 - 0.001)\%$. We show that moving to a high-luminosity regime leads to a significant improvement on the bounds on the top anomalous couplings to a photon or a Z boson.

PACS Numbers: 13.66.-a, 14.65.Ha

Keywords: Top quark, Flavour-Changing Neutral Current, FCC-ee/TLEP

1 Introduction

Top quark with its large mass and very short life time is one of the most interesting discovered particles in the Standard Model (SM). Studying top quark enables us to investigate the electroweak symmetry breaking mechanism (EWSB) as well as searching for extensions of the SM. In the framework of the SM, top-quark Flavour-Changing Neutral Currents (FCNC) only arise at loop level and highly suppressed because of the GIM (Glashow-Iliopoulos-Maiani) mechanism [1]. For example, the SM predictions for the branching fractions of FCNC processes like $t \rightarrow \gamma u(c)$ and $t \rightarrow Zu(c)$ are of the order of 10^{-14} and 10^{-16} , respectively. The ability of the present experiments is far from measuring such tiny branching ratios. On the other hand, several extensions of the SM such as Technicolor, SUSY models, Higgs doublet models predict much higher branching ratios up to $10^8 - 10^{10}$ order of magnitude larger than SM values [2–8]. Consequently, any observation of these rare FCNC transitions would be a clear signal of new physics beyond the SM.

Recently, both CMS and ATLAS experiments have looked for FCNC transitions of the top quark to γ , gluon, Z and Higgs bosons through different channels [9–20]. The most stringent observed upper limits at 95% confidence level (CL) have been found to be [13, 20]:

$$BR(t \rightarrow Zq) < 0.05\% , \quad BR(t \rightarrow u\gamma) < 0.0161\% , \quad BR(t \rightarrow c\gamma) < 0.182\% . \quad (1)$$

The limit on the $t \rightarrow qZ$ has been set using the combination of LHC data at 7 and 8 TeV while the bounds on $t \rightarrow u(c)\gamma$ are based on only 8 TeV data. It is notable to mention here that even at the future upgrades of the LHC, these bounds would not be improved considerably. For example, the future upper bounds on $BR(t \rightarrow qZ)$ have been predicted to be 0.01% at 95% CL at 14 TeV center-of-mass energy with 3000 fb^{-1} of integrated luminosity of data [21, 22]. Therefore, an important task is to look at the future colliders potential to search for the anomalous FCNC couplings, in particular the e^-e^+ colliders such as ILC, CLIC and the Future Circular Collider (FCC) [23–29]. In [30], an analysis has been performed to probe the sensitivity of a future e^-e^+ collider to top FCNC to the photon and a Z boson in the $e^-e^+ \rightarrow Z/\gamma \rightarrow t\bar{q}$ ($\bar{t}q$) channel. This analysis has been done at the center-of-mass energies of 500 GeV and 800 GeV with the integrated luminosity of up to 1000 fb^{-1} without including parton showering, hadronization, and decay of unstable particles. However, the analysis considers cases with no beam polarization, with polarization of electron and with the case of polarization of electron and positron. Then the sensitivity to $tq\gamma$ and tqZ FCNC couplings have been estimated.

The future large scale circular electron-positron collider (FCC-ee) would be one of the high-precision and high-luminosity machines which will be able to perform precise measurements on the Higgs boson, top-quark, Z and W bosons [31, 32]. Due to the expected large amount of data and large production rates, FCC-ee can provide an excellent opportunity for precise studies, in particular in the top quark sector. FCC-ee is designed to be working at the center-of-mass energy up to the $t\bar{t}$ threshold mass, i.e. $\sqrt{s} = 350 \text{ GeV}$ which is upgradeable to 500 GeV. The goal is to reach to a luminosity of $L = 1.3 \times 10^{34} \text{ cm}^{-2}\text{s}^{-1}$ [31, 32].

In this paper, our aim is to study the anomalous FCNC of $tq\gamma$ and tqZ via single top quark production in the FCC-ee at three different center-of-mass energies of 240 GeV, 350 GeV and 500 GeV. The final state consists of a top quark in association with a light-quark. We consider the leptonic decay of the W boson in top quark decay, ($t \rightarrow Wb \rightarrow \ell\nu_\ell b$). In the analysis, we perform parton shower, hadronization and decays of unstable particles as well as a raw detector simulation. We present the 3σ discovery ranges and upper limits on the branching ratios at 95% C.L in terms of the integrated luminosity. Finally, the results are compared with the present and future results from the LHC experiments

The paper is organized as follows. In Section 2 we present the theoretical framework which describes the top quark FCNC couplings to a photon and Z boson. The Monte Carlo event generation, detector simulation and signal separation from backgrounds are described in Section 3. In Section 4, the results of the sensitivity estimation are presented. Finally, Section 5 concludes the paper.

2 Theoretical formalism

The anomalous FCNC couplings of a top quark with a photon and Z boson can be written in a model independent way using an effective Lagrangian approach. The lowest order terms describing $tq\gamma$ and tqZ couplings has the following form [17, 33–36]:

$$\begin{aligned} \mathcal{L}_{eff} = \sum_{q=u,c} & \left[e\lambda_{tq}\bar{t}(\lambda^v - \lambda^a\gamma^5)\frac{i\sigma_{\mu\nu}q^\nu}{m_t}qA^\mu \right. \\ & + \frac{g_W}{2c_W}\kappa_{tq}\bar{t}(\kappa^v - \kappa^a\gamma^5)\frac{i\sigma_{\mu\nu}q^\nu}{m_t}qZ^\mu \\ & \left. + \frac{g_W}{2c_W}X_{tq}\bar{t}\gamma_\mu(x^L P_L + x^R P_R)qZ^\mu \right] + \text{h.c.}, \end{aligned} \quad (2)$$

where the λ_{tq} , κ_{tq} and X_{tq} are dimensionless real parameters that denote the strength of the anomalous FCNC couplings. In the effective Lagrangian, the complex chirality parameters are normalized to $|\lambda^a|^2 + |\lambda^v|^2 = |x^L|^2 + |x^R|^2 = |\kappa^v|^2 + |\kappa^a|^2 = 1$ and $P_{L,R}$ are the left- and right-handed projection operators, $P_{L,R} = \frac{1}{2}(1 \mp \gamma^5)$. It is notable that the term which contains γ^μ is dimension four and the terms with $\sigma^{\mu\nu}$ are dimension five. The anomalous FCNC interactions $tq\gamma$ and tqZ lead to production of a top quark in association with a light quark in electron-positron collisions. The Feynman diagram for this process is shown in Figure 1 including the subsequent leptonic decay of the W boson in top quark decay. In Table 1, the cross sections of $e^- + e^+ \rightarrow t\bar{u} + t\bar{c} + \bar{t}u + \bar{t}c$ including the branching ratio of top quark decays into a W boson and a b -quark with W boson decays into a charged lepton (muon and electron) and neutrino are presented. The cross sections are shown at three different center-of-mass energies of 240, 350 and 500 GeV. It should be pointed out that the cross sections due to photon and Z boson exchange are different and depends on the type of coupling. The contribution of photon exchange and Z boson with $\sigma^{\mu\nu}$ coupling increases with the energy of the center-of-mass. This is because of the presence of an additional momentum factor q^ν in the effective Lagrangian.

According to the three independent terms of the Lagrangian, there are three separate ways to produce single top quark plus a light quark. In this analysis, all three terms of the Lagrangian are investigated independently with the following sets of the parameters: $\lambda^v = 1, \lambda^a = 0$ for $tq\gamma$, for vector like coupling of tqZ : $x^L = x^R = 1$ while for tensor FCNC coupling of tqZ : $\kappa^v = 1, \kappa^a = 0$. In case of observing an excess indicating FCNC signal, the angular distribution of the outgoing particles can be used to determine the chirality of the FCNC couplings. In Figure 2, the distributions of the cosine of the angle between the outgoing charged lepton with respect to the z -axis (beam axis) are depicted for the $tq\gamma$ signal scenario with three independent types of couplings: $(\lambda^v = 1, \lambda^a = 0)$, $(\lambda^v = 1, \lambda^a = 1)$ and $(\lambda^v = 1, \lambda^a = -1)$. As it can be seen, for the type of coupling with no γ^5 , the angular distribution is quite flat while for the type of coupling with projection operator $1 \pm \gamma^5$ the distribution has a behaviour like a parabola with opposite shapes depending on the sign of γ^5 .

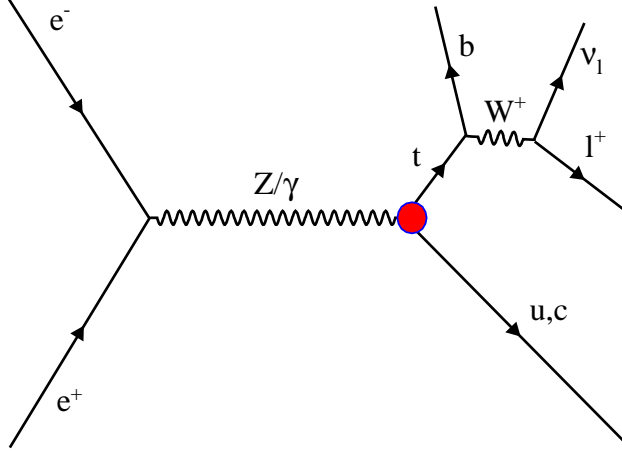


Figure 1: The Feynman diagram for production of a top in association with a light quark due to the anomalous couplings $tq\gamma$ and tqZ in electron-positron collisions.

\sqrt{s}	240 GeV		350 GeV		500 GeV	
FCNC couplings	$\sigma(\text{fb})$ Signal	$\sigma(\text{fb})$ Bkg.	$\sigma(\text{fb})$ Signal	$\sigma(\text{fb})$ Bkg.	$\sigma(\text{fb})$ Signal	$\sigma(\text{fb})$ Bkg.
$tq\gamma$	$2154(\lambda_{tq})^2$	4879	$3832(\lambda_{tq})^2$	3221.2	$4302(\lambda_{tq})^2$	2048.6
tqZ ($\sigma_{\mu\nu}$)	$1434(\kappa_{tq})^2$	4879	$2160(\kappa_{tq})^2$	3221.2	$2282(\kappa_{tq})^2$	2048.6
tqZ (γ_μ)	$916(X_{tq})^2$	4879	$786(X_{tq})^2$	3221.2	$464(X_{tq})^2$	2048.6

Table 1: Cross-sections (in fb) of $\sigma(e^- + e^+ \rightarrow t\bar{u} + t\bar{c} + \bar{t}u + \bar{t}c) \times Br(t \rightarrow Wb \rightarrow l\nu b)$ with $l = e, \mu$ for three signal scenarios, $tq\gamma$, tqZ (vector-tensor) before applying cuts. The cross section of the main background process $W^\pm jj$ including the branching ratio of the leptonic decay of the W boson is also presented.

3 Analysis strategy

As we have mentioned before, this study is dedicated to probe the $tq\gamma$ and tqZ FCNC couplings via single top quark production at FCC-ee. The results will be presented at different center-of-mass energies of the colliding electron-positron. In this section, the details of the event generation and Monte Carlo simulation for signal and background, event selection, and multivariate analysis to separate signal from SM background will be presented.

3.1 Event generation and simulation

Now, we present the signal and the corresponding backgrounds generation in the e^-e^+ collisions. The signal is defined as $e^-e^+ \rightarrow Z/\gamma \rightarrow t\bar{q}$ ($\bar{t}q$), where q is an up or a charm quark. The top quark decays through SM, $t \rightarrow W^+b \rightarrow \ell^+\nu_\ell b$ and $\bar{t} \rightarrow W^-\bar{b} \rightarrow \ell^-\bar{\nu}_\ell \bar{b}$. Therefore, the final state consists of a charged lepton, missing energy, a b-jet and a light jet.

In order to simulate and generate the signal events, the effective Lagrangian describing the FCNC couplings is implemented with the FEYNRULES package [37–41], then the model has been imported to a UFO module [42] and inserted in MADGRAPH 5 [43, 44].

Based on the expected signature of the signal events, the main background contribution is

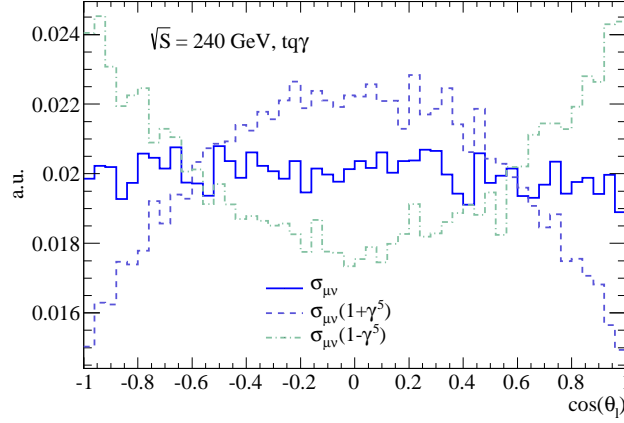


Figure 2: The distribution of the cosine of the angle between the outgoing charged lepton with the z -axis for $tq\gamma$ with different chirality at the center-of-mass energy of 240 GeV.

originating from WW production when one of the W bosons decays hadronically and another one decays leptonically, i.e. $e^+e^- \rightarrow W^+W^- \rightarrow \ell^+\nu_\ell jj(\ell^-\bar{\nu}_\ell jj)$. Again, we use MADGRAPH 5 to generate the background events. The signal and background events are generated in the center-of-mass energies of $\sqrt{s}=240, 350$ and 500 GeV.

We employ PYTHIA 8.1 package [45–48] for parton showering, hadronization and decay of unstable particles. To reconstruct jet the FASTJET package [49–51] with an anti- k_t algorithm [52,53] with a cone size of $R = 0.4$ is used. Where $R = \sqrt{(\Delta\eta)^2 + (\Delta\phi)^2}$, with $\eta = -\ln(\tan(\theta/2))$. The parameters ϕ and η are the azimuthal and polar angles with respect to the z -axis. We present the results with 70% for the efficiency of b-tagging and a 5% mistagging rates is also considered. In our analysis, b-tagging plays an important role to reject the contribution of WW background. More background rejection affects the final upper limits on the branching ratios.

To account for the detector resolution, the final state particles (leptons and jets) are smeared according to a Gaussian distribution with the following parameterization [54,55]:

$$\frac{\Delta E_j}{E_j} = \frac{40\%}{\sqrt{E_j \text{ (GeV)}}} \oplus 2.5\%, \quad \frac{\Delta E_\ell}{E_\ell} = \frac{15\%}{\sqrt{E_\ell \text{ (GeV)}}} \oplus 1\%, \quad (3)$$

where ℓ stands for lepton which can be an electron or a muon and j stands for final state jets. The symbol \oplus represents a quadrature sum. In reality, the electron and muon energy resolutions show different dependencies on the electromagnetic calorimetry and tracking of charged particle. Nevertheless, in our analysis the uniform values for energy resolution are used for the final state lepton. It is a more conservative assumption for the energies under consideration in this analysis than the capabilities of tracking. Now, we apply the following detector acceptance cuts on the final state objects:

$$p_T^{jet,b-jet} \geq 20 \text{ GeV}, \quad p_T^\ell \geq 10 \text{ GeV}, \quad \cancel{E}_T^{miss} \geq 20 \text{ GeV}, \quad |\eta^{jet,\ell,b-jet}| < 2.5, \quad (4)$$

where $p_T^{jet,\ell,b-jet}$ are the transverse momenta of jets, leptons and b-quark jet, respectively. \cancel{E}_T^{miss} is the missing transverse energy. In addition to these cuts, to have well separated objects, we require the distances in the (η, ϕ) space between each two objects to be greater than 0.4. The presence of a charged lepton (electron or muon) with $p_T^\ell \geq 10 \text{ GeV}$ and $|\eta^\ell| < 2.5$, which is tagged as originating from W boson decay, is required for the leptonic decays channel of top quark.

In order to reconstruct the top quark, all components of the neutrino momentum is needed. The missing transverse energy (\cancel{E}_T^{miss}) is taken as the transverse component of neutrino momentum. We obtain the z-component of the neutrino momentum by using the W boson mass constraint: $M_W^2 = (p_\ell + p_\nu)^2$. In most cases, two solutions are obtained for the z-component of the neutrino. Consequently, the combination of the charged lepton and two neutrinos gives two W bosons, which is combined with the highest- p_T b-tagged jet. The combination which leads to closest mass to the top quark mass is then chosen. Among all reconstructed untagged jets, the one with highest- p_T is chosen to be jet originating from the light quark in the signal final state. Finally, the mass distribution of the reconstructed top-quark is illustrated in Figure 3 for $tq\gamma$ signal and for $W^\pm jj$ SM background. These distributions are at the center-of-mass energy of 350 GeV. It is worth mentioning that as expected the signal distribution has a peak near the top mass while the background events have an almost flat distribution with no peak. Moving to higher center-of-mass energies causes to more separation of top mass distributions of signal from background.

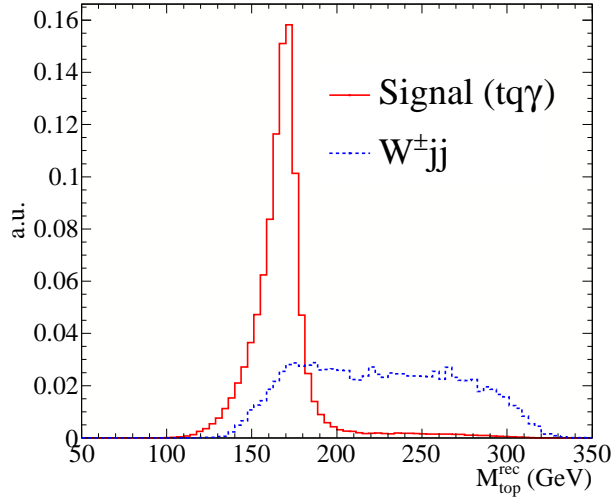


Figure 3: The normalized reconstructed top quark mass distributions for signal ($tq\gamma$) and corresponding background at $\sqrt{s} = 350$ GeV. The signal has been shown with $\lambda_{tq} = 0.1$.

\sqrt{s}	240 GeV		350 GeV		500 GeV	
FCNC couplings	$\sigma(\text{fb})$ Signal	$\sigma(\text{fb})$ Bkg.	$\sigma(\text{fb})$ Signal	$\sigma(\text{fb})$ Bkg.	$\sigma(\text{fb})$ Signal	$\sigma(\text{fb})$ Bkg.
$tq\gamma$	$1078.4(\lambda_{tq})^2$	2083.3	$1899.2(\lambda_{tq})^2$	1230.5	$2095(\lambda_{tq})^2$	702.7
tqZ ($\sigma_{\mu\nu}$)	$714.3(\kappa_{tq})^2$	2083.3	$1067(\kappa_{tq})^2$	1230.5	$1109(\kappa_{tq})^2$	702.7
tqZ (γ_μ)	$458(X_{tq})^2$	2083.3	$386(X_{tq})^2$	1230.5	$226(X_{tq})^2$	702.7

Table 2: Cross-sections (in fb) for three signal scenarios, $tq\gamma$, tqZ (vector and tensor) after including the branching ratios and after applying the preliminary kinematic cuts.

3.2 Separation of signal from background

In order to reduce the main SM background $W^\pm jj$ which have a different topology than the signal events, a multivariate technique [57–61] is used. After the pre-selection cuts described in the previous section which consists of detector acceptance cuts, b -tagging efficiency and misidentification rate around 48–50% of the signal events and about 35–40% of background events are survived. The cross sections of signal in all scenarios and backgrounds at three center-of-mass energies after the pre-selection cuts are presented in Table 2.

These pre-selection cuts are generally loose selections on single variables, which remove a large fraction of the background events while barely reducing also the signal events. Then in order to obtain a better separation of signal from background events, a multivariate technique is used. The choice of proper set of variables is very efficient in surviving the signal, while reducing the large fraction of SM background events. We select those variables which have the best possible discrimination power between signal and background. The following variables are used in the analysis:

- The angular separation between the reconstructed W boson and b -jet, $\Delta R(W, b - jet)$
- the transverse momentum and pseudorapidity distribution of the b -jet, $p_T^{b-jet}, \eta^{b-jet}$
- the reconstructed top mass, M_{top}^{rec}
- the energy and pseudorapidity of the charged lepton, E^ℓ, η^ℓ
- the transverse momentum of reconstructed top-quark, P_T^{top}
- the energy of the light jets, E^{jets}

The kinematic distributions of some of these variables are shown in Figures 4. These distributions are corresponding to the signal scenario with anomalous $tq\gamma$ couplings at the center-of-mass energy of 350 GeV. For all signal scenarios $tq\gamma$, $tqZ(\gamma^\mu)$ and $tqZ(\sigma_{\mu\nu})$ the same variables are used while multivariate analyses are different because of different behaviours in shapes of these variables. The analyses are performed separately at the center-of-mass energies of 240, 350 and 500 GeV. It is remarkable that in this analysis, the events with only one b -tagged jet are kept and the total number of jets is free to be two or three. These requirements with the preliminary requirement of the presence of only one isolated charged lepton in the final state help suppress the contribution of background events from top pair production.

The cross sections of the signals $tq\gamma$ and $tqZ(\gamma_\mu, \sigma_{\mu\nu})$ and the main background $W^\pm jj$ after performing the multivariate analysis are presented in Table 3. As it be seen from the Table 3, the background rejection rate varies at different center-of-mass energies. For all signal scenarios, the background rejection rates are $\sim 10^{-1}$, $\sim 10^{-2}$ and $\sim 10^{-3}$ at the center-of-mass energies of 240, 350, 500 GeV, respectively. The discriminating power of the input variables are increasing with the center-of-mass energies of the collision. When we go to higher energies the overlapping between the signal and background distributions reduces. In particular, this happens for the top mass, lepton energy and top quark transverse momentum distributions. Larger background suppression is achieved for the tqZ signal with $\sigma_{\mu\nu}$ coupling. Since the signal-to-background ratio for all signal scenarios increases with the increment of the center-of-mass energy, more sensitivity is expected at larger energies.

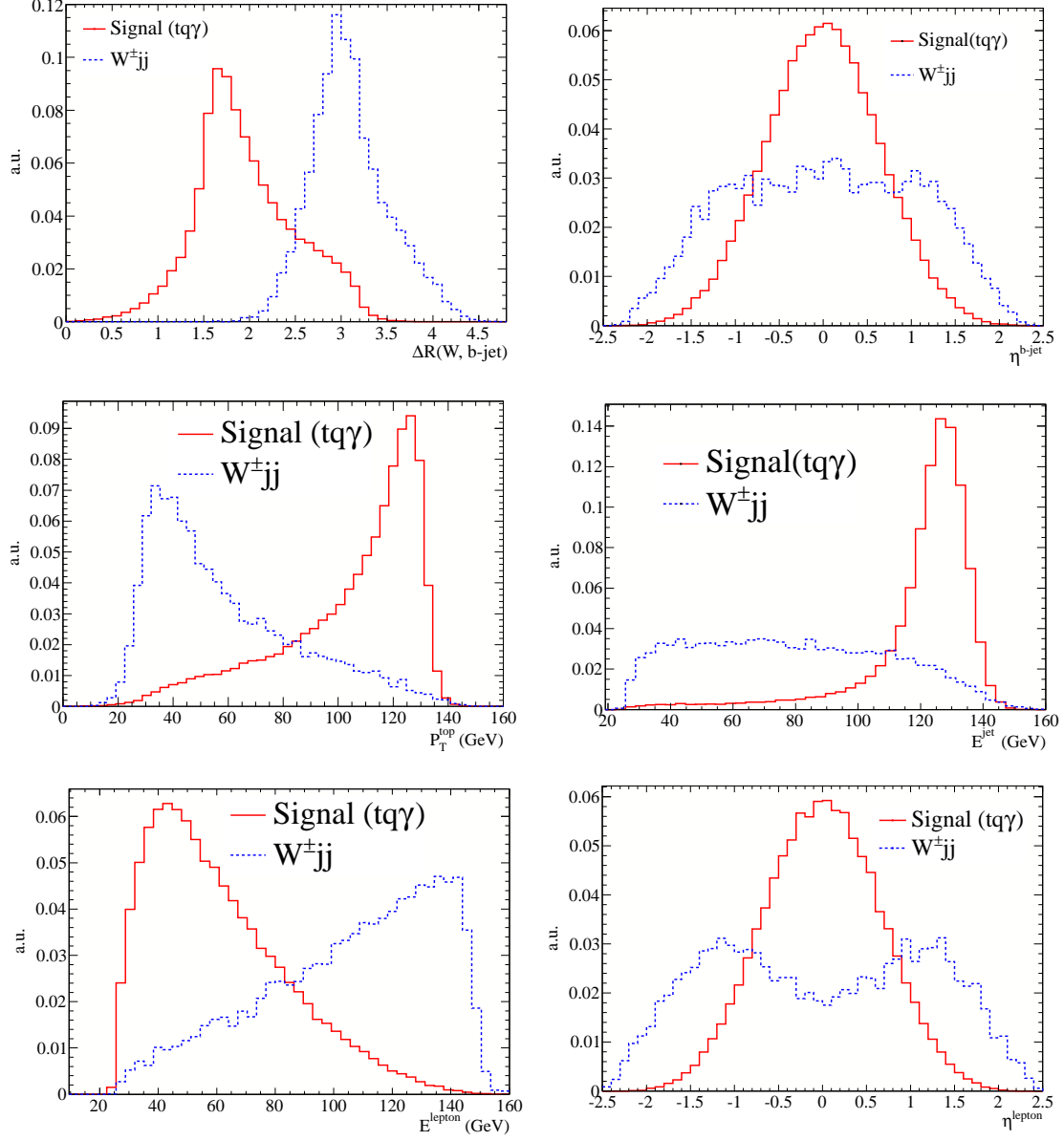


Figure 4: The normalized kinematic distributions of the input variables in multivariate analysis for the collisions at the center-of-mass energy of 350 GeV.

\sqrt{s}	240 GeV		350 GeV		500 GeV	
FCNC couplings	$\sigma(\text{fb})$ Signal	$\sigma(\text{fb})$ Bkg.	$\sigma(\text{fb})$ Signal	$\sigma(\text{fb})$ Bkg.	$\sigma(\text{fb})$ Signal	$\sigma(\text{fb})$ Bkg.
$tq\gamma$	$1027.7(\lambda_{tq})^2$	54.1	$1866.1(\lambda_{tq})^2$	6.1	$2091.4(\lambda_{tq})^2$	0.74
$tqZ (\sigma_{\mu\nu})$	$688.7(\kappa_{tq})^2$	69.7	$1057.4(\kappa_{tq})^2$	6.3	$1106.5(\kappa_{tq})^2$	0.59
$tqZ (\gamma_\mu)$	$436.5(X_{tq})^2$	56.1	$383.6(X_{tq})^2$	6.7	$223.8(X_{tq})^2$	1.31

Table 3: Cross-sections (in fb) for three signal scenarios, $tq\gamma$, tqZ (vector and tensor) after performing the multivariate analysis to separate signal from background events.

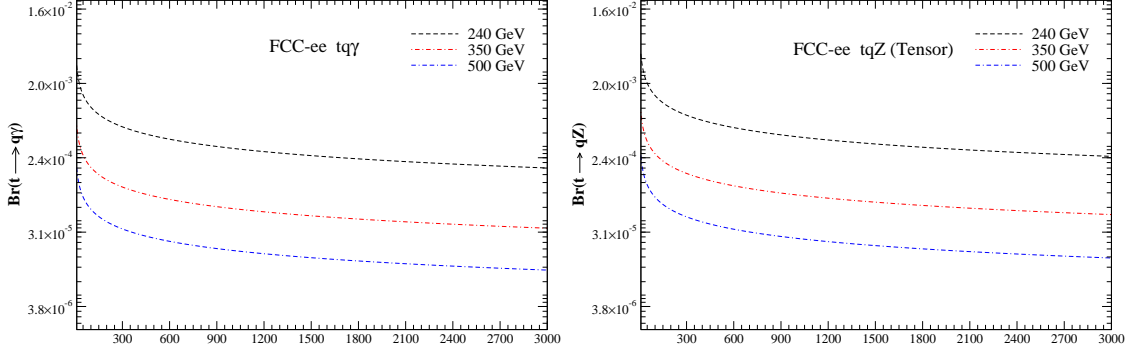
4 Sensitivity estimation

For estimation of the FCNC sensitivity, the expected 3σ significance and the upper limits on the anomalous couplings and the branching ratios at 95% C.L are presented. The 3σ discovery ranges are obtained using the significance S/\sqrt{B} where S and B are the number of signal and background events after all selections, respectively. The number of signal and background events can be obtained by: $S = \sigma_{\text{signal}} \times \mathcal{L}$ and $B = \sigma_{\text{bkg}} \times \mathcal{L}$. The cross sections of signal and backgrounds are taken from Table 3 which are the obtained after all selection cuts. Without including any systematic effects, the 3σ discovery regions of the branching ratios are presented in Table 4 for three signal scenarios at three center-of-mass energies of the electron-positron collision. The 3σ discovery regions in terms of the integrated luminosity are also depicted in Figure 5. We observe that at 3σ significance level branching ratios at the order of 10^{-3} is achievable at the center-of-mass energy of 240 GeV while going to larger energies of 350 and 500 GeV leads to an improvement of one order of magnitude for $tq\gamma$ and $tqZ(\sigma_{\mu\nu})$ with an integrated luminosity of 100 fb^{-1} . The FCNC transition of $t \rightarrow qZ$ with γ_μ -type couplings would not be measured better than the order of 10^{-4} . This is because of the lack of a momentum factor q^ν in the effective Lagrangian with respect to the other signal scenarios that causes to lower signal cross section. According to Figure 5, going to high luminosity regime at the center-of-mass energies of 240 and 350 leads to a reach sensitivity at the order of 10^{-5} . To achieve a better sensitivity of the order of 10^{-6} , we need to increase the center-of-mass energy of 500 GeV.

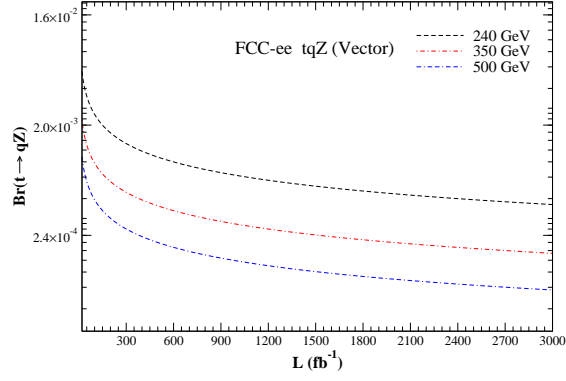
\sqrt{s} (GeV)	240	350	500
$Br(t \rightarrow q\gamma)$	1.0×10^{-3}	1.9×10^{-4}	5.8×10^{-5}
$Br(t \rightarrow qZ) (\sigma_{\mu\nu})$	1.7×10^{-3}	3.3×10^{-4}	9.7×10^{-5}
$Br(t \rightarrow qZ) (\gamma_\mu)$	2.4×10^{-3}	9.5×10^{-4}	7.2×10^{-4}

Table 4: The sensitivity for a significance level of 3σ at the center-of-mass energies of 240, 350, 500 GeV and with 100 fb^{-1} of integrated luminosity of data.

In order to set 95% C.L upper limits on the anomalous FCNC couplings and consequently on the branching ratios, the CLs procedure is used [62]. The CLs technique is currently used by the big experiments such as ATLAS and CMS experiments to provide upper limits on the new physics cross sections and constraining the theory parameters. For the limits calculations the RooStats [63] package has been used. The 95% C.L upper limits on the branching ratios of $t \rightarrow q\gamma$ and $t \rightarrow qZ$ at the center-of-mass energies of 240, 350 and 500 GeV are shown in Table 5 based on an integrated luminosity of 100 fb^{-1} . As we expected, at each center-of-mass energy,



(a)



(c)

Figure 5: Branching ratios of a FCNC signal detectable at the 3σ level as a function of integrated luminosity at $\sqrt{s} = 240, 350$ and 500 GeV of FCC-ee energies. (a) for $Br(t \rightarrow q\gamma)$, (b) for $Br(t \rightarrow qZ)$ ($\sigma_{\mu\nu}$), and (c) for $Br(t \rightarrow qZ)$ (γ_μ).

the loosest limits belong to the FCNC transition of $t \rightarrow qZ$ with γ_μ -type coupling ($10^{-3} - 10^{-4}$). We note that the larger center-of-mass energy leads to even the level of one order of magnitude tighter bounds.

In Figure 6, we present the current observed upper limits on the $Br(t \rightarrow qZ)$ versus $Br(t \rightarrow q\gamma)$ at 95% C.L from the recent analyses of the ATLAS and CMS experiments. The expected sensitivity from the ATLAS experiment with 300 fb^{-1} is in proton-proton collisions at the center-of-mass energy of 14 TeV is also shown by the dashed lines. The sensitivity of the FCC-ee with 100 fb^{-1} at the center-of-mass energy of 350 GeV is compared with the CMS and ATLAS results. With an integrated luminosity of 300 fb^{-1} , ATLAS is expected to reach to an upper limit of 7.8×10^{-5} on the branching ratio of $t \rightarrow q\gamma$ and 2.3×10^{-4} on the branching ratio of $t \rightarrow qZ$ ($\sigma_{\mu\nu}$ -type coupling). The FCC-ee potential upper limits are expected to be significantly smaller than the attainable limits by the future LHC program.

\sqrt{s} (GeV)	240	350	500
$Br(t \rightarrow q\gamma)$	5.9×10^{-4}	2.3×10^{-5}	8.9×10^{-6}
$Br(t \rightarrow qZ) (\sigma_{\mu\nu})$	8.8×10^{-4}	6.7×10^{-5}	1.4×10^{-5}
$Br(t \rightarrow qZ) (\gamma_\mu)$	1.4×10^{-3}	1.9×10^{-4}	8.4×10^{-5}

Table 5: The upper limits on the top FCNC decays at 95% C.L obtained using the CLs method at the center-of-mass energies of 240, 350 and 500 GeV based on an integrated luminosity of 100 fb^{-1} .

It is worth mentioning that the FCNC transitions can also be probed in $t\bar{t}$ production when a top quark decays anomalously into $q+\gamma$ or $q+Z$. However, it has been found that the limits would be looser than the ones obtained in single top productions [64]. It is remarkable that although the limits obtained in this study are expected to be more stringent than the LHC future however in case of observing the signal, in contrary to FCC-ee, LHC is able to discriminate between anomalous $tq\gamma$ and tqZ . In case of signal observation, LHC would also be able to discriminate between anomalous tuV and tcV using for example the charge ratio technique [65]. This also would be possible at the FCC-ee in case of having detectors with good efficiency of charm tagging.

5 Summary and conclusions

Top quark flavor-changing neutral current interactions are extremely forbidden in the SM framework because of the GIM (Glashow-Iliopoulos-Maiani) mechanisms. The SM predictions for branching ratios of the top quark decay into a photon or a Z boson and an up-type quark are at the order of 10^{-14} . However, several extensions of the SM can enhance the branching ratios by a factor of 10^{8-9} depending on the model. Therefore, precise measurement of these branching ratios provide an excellent possibility to probe the extensions of SM in the top quark sector. While it is impossible to measure the branching ratios with the precisions of order of 10^{-14} to test the SM, observation of sizeable branching ratios would indicate new physics beyond the SM.

FCC-ee/TLEP with a clean environment and large luminosity would provide a unique opportunity to measure the properties of particles and their interactions. In this work, we investigate the sensitivity and discovery prospects of FCC-ee/TLEP to the top quark FCNC transitions. We look for the FCNC $tq\gamma$ and tqZ couplings in single top-quark production in the process of $e^- + e^+ \rightarrow t\bar{q} + \bar{t}q$. We perform the analysis in a model independent way using the effective Lagrangian approach at the center-of-mass energies of $\sqrt{s} = 240, 350$ and 500 GeV . In the analysis,

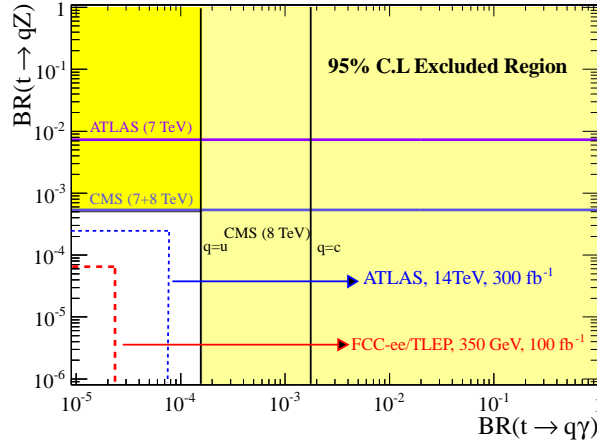


Figure 6: The current observed upper limits on the $Br(t \rightarrow qZ)$ versus $Br(t \rightarrow q\gamma)$ at 95% C.L from the recent analyses of the ATLAS and CMS experiments. The expected sensitivity from the ATLAS experiment with 300 fb^{-1} is also shown by the dashed lines. The sensitivity of the FCC-ee with 100 fb^{-1} at the center-of-mass energy of 350 GeV is presented as well.

we only consider the leptonic (electron and muon) decay of the W boson in the top quark decay. In the analysis, parton shower, hadronization and decay of unstable particles are performed using PYTHIA and jets are reconstructed using the anti- k_t algorithm available in the FASTJET package. The main background arises from the WW events, with one W boson decays leptonically. A set of kinematic variables has been proposed as the input variables to a multivariate analysis for discrimination between signal from background events. We find the 3σ discovery ranges and the 95% C.L sensitivity for three signal scenarios versus the integrated luminosity at the center-of-mass energies of 240, 350 and 500 GeV. We find that with increasing the center-of-mass energy stronger bounds would be reachable. With an integrated luminosity of 100 fb^{-1} at the center-of-mass energy of 350 GeV, upper limits of 2.3×10^{-5} , 6.7×10^{-5} would be obtained on $Br(t \rightarrow q\gamma)$ and $Br(t \rightarrow qZ)$ ($\sigma_{\mu\nu}$ -type), respectively. A looser upper limit of 1.9×10^{-4} on $Br(t \rightarrow qZ)$ with γ_μ -type interaction is obtained. It is found that a sensitivity of the order of 10^{-6} at large integrated luminosities would be attainable. The results are compared with the expected LHC results at the center-of-mass energy of 14 TeV with 300 fb^{-1} . FCC-ee will be able to reach a considerable sensitivity to the anomalous FCNC couplings of $tq\gamma$ and tqZ . Finally, it is remarkable that in all signal scenarios and even with large amount of data $\sim 3 \text{ ab}^{-1}$, the branching ratios would not be measured better than 10^{-6} .

References

- [1] S. L. Glashow, J. Iliopoulos and L. Maiani, Phys. Rev. D **2**, 1285 (1970).
- [2] K. Agashe *et al.* [Top Quark Working Group Collaboration], arXiv:1311.2028 [hep-ph].
- [3] S. Bejar, J. Guasch, D. Lopez-Val and J. Sola, Phys. Lett. B **668**, 364 (2008) [arXiv:0805.0973 [hep-ph]].
- [4] J. Cao, Z. Heng, L. Wu and J. M. Yang, Phys. Rev. D **79**, 054003 (2009), [arXiv:0812.1698 [hep-ph]];

- R. Guedes, R. Santos and M. Won, arXiv:1308.4723 [hep-ph].
- [5] G. A. Gonzalez-Sprinberg and R. Martinez, hep-ph/0605335;
R. Coimbra, A. Onofre, R. Santos and M. Won, Eur. Phys. J. C **72**, 2222 (2012) [arXiv:1207.7026 [hep-ph]].
 - [6] R. A. Diaz, R. Martinez and J. Alexis Rodriguez, hep-ph/0103307.
 - [7] G. -r. Lu, F. -r. Yin, X. -l. Wang and L. -d. Wan, Phys. Rev. D **68**, 015002 (2003) [hep-ph/0303122].
 - [8] G. Couture, M. Frank and H. Konig, Phys. Rev. D **56**, 4213 (1997) [hep-ph/9704305].
 - [9] The ATLAS collaboration, ATLAS-CONF-2013-063.
 - [10] G. Aad *et al.* [ATLAS Collaboration], JHEP **1406**, 008 (2014) [arXiv:1403.6293 [hep-ex]].
 - [11] S. Chatrchyan *et al.* [CMS Collaboration], Phys. Lett. B **718**, 1252 (2013) [arXiv:1208.0957 [hep-ex]].
 - [12] G. Aad *et al.* [ATLAS Collaboration], JHEP **1209**, 139 (2012) [arXiv:1206.0257 [hep-ex]].
 - [13] S. Chatrchyan *et al.* [CMS Collaboration], Phys. Rev. Lett. **112**, 171802 (2014) [arXiv:1312.4194 [hep-ex]].
 - [14] Y. Chao [CMS Collaboration], PoS EPS **-HEP2013**, 069 (2014).
 - [15] V. M. Abazov *et al.* [D0 Collaboration], Phys. Lett. B **701**, 313 (2011) [arXiv:1103.4574 [hep-ex]].
 - [16] H. Abramowicz *et al.* [ZEUS Collaboration], Phys. Lett. B **708**, 27 (2012) [arXiv:1111.3901 [hep-ex]].
 - [17] V. F. Obraztsov, S. R. Slabospitsky and O. P. Yushchenko, Phys. Lett. B **426**, 393 (1998) [hep-ph/9712394].
 - [18] P. Achard *et al.* [L3 Collaboration], Phys. Lett. B **549**, 290 (2002) [hep-ex/0210041].
 - [19] J. Abdallah *et al.* [DELPHI Collaboration], Phys. Lett. B **590**, 21 (2004) [hep-ex/0404014].
 - [20] CMS Collaboration [CMS Collaboration], CMS-PAS-TOP-14-003.
 - [21] CMS PAS FTR-13-016.
 - [22] ATLAS Collaboration, ATL-PHYS-PUB-2012-001.
 - [23] H. Abramowicz *et al.* [CLIC Detector and Physics Study Collaboration], arXiv:1307.5288 [hep-ex].
 - [24] D. Asner, A. Hoang, Y. Kiyo, R. Pschl, Y. Sumino and M. Vos, arXiv:1307.8265 [hep-ex].
 - [25] "Miyamoto, Akiya and Stanitzki, Marcel and Weerts, Harry and Linssen, Lucie", Report", [arXiv:1202.5940], CERN-2012-003. ANL-HEP-TR-12-01. DESY-12-008. KEK-Report-2011-7,

- [26] P. Lebrun, L. Linssen, A. Lucaci-Timoce, D. Schulte, F. Simon, S. Stapnes, N. Toge and H. Weerts *et al.*, arXiv:1209.2543 [physics.ins-det].
- [27] MAicheler, MAicheler, PBurrows, MDraper, TGarvey, PLebrun, KPeach and NPhinney *et al.*, CERN-2012-007.
- [28] J. E. Brau, R. M. Godbole, F. R. L. Diberder, M. A. Thomson, H. Weerts, G. Weiglein, J. D. Wells and H. Yamamoto, arXiv:1210.0202 [hep-ex].
- [29] M. Martinez and R. Miquel, Eur. Phys. J. C **27**, 49 (2003) [hep-ph/0207315].
- [30] J. A. Aguilar-Saavedra, Phys. Lett. B **502**, 115 (2001) [hep-ph/0012305];
- [31] M. Bicer *et al.* [TLEP Design Study Working Group Collaboration], JHEP **1401**, 164 (2014) [arXiv:1308.6176 [hep-ex]].
- [32] M. Koratzinos, A. P. Blondel, R. Aleksan, O. Brunner, A. Butterworth, P. Janot, E. Jensen and J. Osborne *et al.*, arXiv:1305.6498 [physics.acc-ph].
- [33] E. Malkawi and T. M. P. Tait, Phys. Rev. D **54**, 5758 (1996) [hep-ph/9511337];
Y. .P. Gouz and S. R. Slabospitsky, Phys. Lett. B **457**, 177 (1999) [hep-ph/9811330].
- [34] M. Hosch, K. Whisnant and B. L. Young, Phys. Rev. D **56**, 5725 (1997) [hep-ph/9703450];
J. A. Aguilar-Saavedra, Nucl. Phys. B **812**, 181 (2009) [arXiv:0811.3842 [hep-ph]].
- [35] J. A. Aguilar-Saavedra, Nucl. Phys. B **837**, 122 (2010) [arXiv:1003.3173 [hep-ph]].
- [36] J. A. Aguilar-Saavedra, Acta Phys. Polon. B **35**, 2695 (2004) [hep-ph/0409342].
- [37] A. Alloul, N. D. Christensen, C. Degrande, C. Duhr and B. Fuks, Comput. Phys. Commun. **185**, 2250 (2014) [arXiv:1310.1921 [hep-ph]].
- [38] N. D. Christensen, C. Duhr, B. Fuks, J. Reuter and C. Speckner, Eur. Phys. J. C **72**, 1990 (2012) [arXiv:1010.3251 [hep-ph]].
- [39] B. Fuks, Int. J. Mod. Phys. A **27**, 1230007 (2012) [arXiv:1202.4769 [hep-ph]].
- [40] C. Duhr and B. Fuks, Comput. Phys. Commun. **182**, 2404 (2011) [arXiv:1102.4191 [hep-ph]].
- [41] N. D. Christensen, P. de Aquino, C. Degrande, C. Duhr, B. Fuks, M. Herquet, F. Maltoni and S. Schumann, Eur. Phys. J. C **71**, 1541 (2011) [arXiv:0906.2474 [hep-ph]].
- [42] C. Degrande, C. Duhr, B. Fuks, D. Grellscheid, O. Mattelaer and T. Reiter, Comput. Phys. Commun. **183**, 1201 (2012) [arXiv:1108.2040 [hep-ph]].
- [43] J. Alwall, M. Herquet, F. Maltoni, O. Mattelaer and T. Stelzer, JHEP **1106**, 128 (2011) [arXiv:1106.0522 [hep-ph]].
- [44] J. Alwall, R. Frederix, S. Frixione, V. Hirschi, F. Maltoni, O. Mattelaer, H. -S. Shao and T. Stelzer *et al.*, arXiv:1405.0301 [hep-ph].
- [45] P. Skands, S. Carrazza and J. Rojo, arXiv:1404.5630 [hep-ph].
- [46] K. Kong, arXiv:1208.0035 [hep-ph].

- [47] J. -P. Guillaud, CERN-CMS-NOTE-2000-070.
- [48] T. Sjostrand, S. Mrenna and P. Z. Skands, JHEP **0605**, 026 (2006) [hep-ph/0603175].
- [49] M. Cacciari, G. P. Salam and G. Soyez, Eur. Phys. J. C **72**, 1896 (2012) [arXiv:1111.6097 [hep-ph]].
- [50] M. Cacciari, hep-ph/0607071.
- [51] M. Cacciari and G. P. Salam, Phys. Lett. B **641**, 57 (2006) [hep-ph/0512210].
- [52] S. Catani, Y. L. Dokshitzer, M. H. Seymour and B. R. Webber, Nucl. Phys. B **406**, 187 (1993).
- [53] S. D. Ellis and D. E. Soper, Phys. Rev. D **48**, 3160 (1993) [hep-ph/9305266].
- [54] L. Linssen, A. Miyamoto, M. Stanitzki, H. Weerts, arXiv:1202.5940 [physics.ins-det].
- [55] J. Brau *et al.* [ILC Collaboration], arXiv:0712.1950 [physics.acc-ph].
- [56] J. Beringer *et al.* [Particle Data Group Collaboration], Phys. Rev. D **86**, 010001 (2012) and 2013 partial update for the 2014 edition.
- [57] A. Hocker, J. Stelzer, F. Tegenfeldt, H. Voss, K. Voss, A. Christov, S. Henrot-Versille and M. Jachowski *et al.*, PoS ACAT , 040 (2007) [physics/0703039 [PHYSICS]].
- [58] J. Stelzer, A. Hocker, P. Speckmayer and H. Voss, PoS ACAT **08**, 063 (2008).
- [59] J. Therhaag [TMVA Core Developer Team Collaboration], AIP Conf. Proc. **1504**, 1013 (2009).
- [60] P. Speckmayer, A. Hocker, J. Stelzer and H. Voss, J. Phys. Conf. Ser. **219**, 032057 (2010).
- [61] J. Therhaag, PoS ICHEP **2010**, 510 (2010).
- [62] A. L. Read, J. Phys. G **28**, 2693 (2002);
B. Mistlberger and F. Dulat, arXiv:1204.3851 [hep-ph].
- [63] L. Moneta *et al.*, The RooStats project, arXiv:1009.1003
- [64] J. A. Aguilar-Saavedra and T. Riemann, In *2nd ECFA/DESY Study 1998-2001* 2428-2450 [hep-ph/0102197].
- [65] S. Khatibi and M. M. Najafabadi, Phys. Rev. D **89**, 054011 (2014) [arXiv:1402.3073 [hep-ph]].